Effects of a Naturally Occurring Compatible Osmolyte on the Internal Dynamics of Ribonuclease A[†]

Aijun Wang,[‡] Andrew D. Robertson,[§] and D. W. Bolen*,[‖]

Department of Biochemistry, Southern Illinois University at Carbondale, Carbondale, Illinois 62901, Department of Biochemistry, University of Iowa, Iowa City, Iowa 52242, and Human Biological Chemistry and Genetics, University of Texas Medical Branch, 5.154 MRB, Galveston, Texas 77555-1052

Received July 24, 1995; Revised Manuscript Received September 19, 1995[⊗]

ABSTRACT: Osmolytes are small organic solutes accumulated intracellularly by many organisms as they adapt to environmental stresses. Compatible osmolytes, a functional class of osmolytes, increase protein stability while having little or no effect on protein function. To investigate the interrelationships between protein stability, function, and internal dynamics, a hydrogen exchange (HX) quench method was established and used to study the effects of sucrose (a typical compatible osmolyte) on the structural fluctuations of ribonuclease A. It was found that the HX rates of the amide protons with intermediate rates are not affected by 1 M sucrose, but the slow-exchanging amide protons exchange even slower in 1 M sucrose. The protection factors of the slow-exchanging protons fall into a comparatively narrow range while those of the intermediate-exchanging protons vary widely. In agreement with the two-process model [Woodward, C. K., & Hilton, B. D. (1980) *Biophys. J. 32,* 561−575], we conclude that for those slow-exchanging amide protons, the exchange occurs mainly from the compact unfolded state ensemble of the protein. The internal dynamics leading to slow exchange involve exposure of large protein surface areas, similar to that which occurs upon the unfolding of protein. Because sucrose opposes such an increase in protein surface area exposure, both the slow HX rates and the protein stability are affected by sucrose. For those amide protons with fast and intermediate HX rates, the exchange occurs mainly from the native state ensemble of the protein. The internal dynamics involved in the exchange are localized without much surface area change, and functionally important structural fluctuations are likely to occur within this dynamic range. As sucrose does not perturb the native state ensemble significantly, it has little or no effect on protein function and the intermediate HX rates. We propose that the above mechanism is general in terms of effects of compatible osmolyte on protein stability, function, and internal dynamics.

The interrelationships between protein stability, function, and internal dynamics play extremely important roles not only in biological processes but also in protein design and engineering. Organisms that live in extreme environments have had to readjust these interrelationships in adapting to either high temperature, dehydration, high osmotic pressure, the presence of denaturants, or a combination of these stresses (Bagnasco et al., 1986; Garcia-Perez & Burg, 1990; Somero, 1986; Yancey et al., 1982). In the face of such denaturing environments, these organisms have evolved a common strategy to enable them to maintain protein stability and biological activity. This strategy involves the intracellular production and accumulation of certain small organic solutes, known collectively as osmolytes. Compatible osmolytes, defined as those osmolytes that have little or no effect on protein function, have been found to increase protein stability substantially (Santoro et al., 1992; Somero, 1986; Timasheff, 1993; Yancey et al., 1982).

How can compatible osmolytes increase protein stability while having little or no effect on protein function? Since the internal dynamics of a protein are intimately associated with both its stability and function, a related question is, what happens to protein internal dynamics in the presence of compatible osmolytes? In an effort to answer the above questions, we have chosen to monitor protein internal dynamics in the presence and absence of osmolytes by means of NMR-detected amide proton hydrogen exchange (HX).[1] HX kinetics are highly sensitive to protein internal dynamics since exchange requires protein structural fluctuations (Englander & Kallenbach, 1984; Roder, 1989). NMR spectroscopy permits the study of the HX kinetics of individual amide protons, thus providing multiple probes of dynamical behavior all along the main chain.

Generally, HX experiments are initiated by dissolving the protein in D_2O, and NMR spectra are collected as a function of time. The HX rate constants of individual amide protons are obtained from consecutive sets of NMR spectra as a function of time (Kim et al., 1993; Kim & Woodward, 1993; Mayo & Baldwin, 1993; Richarz et al., 1979; Wüthrich & Wagner, 1979). We refer to this mode of HX data collection as the tandem method. A major practical problem in the use of the tandem method is that additives in the HX sample need to be deuterated, or present at low concentration. Since molar concentrations of additives are often required, the tandem method is not only expensive but is also impossible

[†] Supported by U.S. Public Health Research Grant GM49760.
[‡] Southern Illinois University.
[§] University of Iowa.
[‖] University of Texas Medical Branch.
[⊗] Abstract published in *Advance ACS Abstracts,* November 1, 1995.

[1] Abbreviations: RNase A, ribonuclease A; HX, hydrogen exchange; PDLA, poly-DL-alanine; 2D NMR, two-dimensional nuclear magnetic resonance; pH*, pH reading in D_2O without correction for the isotope effect on the electrode.

0006-2960/95/0434-15096$09.00/0

when the additives are unavailable in deuterated forms. In order to study the protein internal dynamics in the presence of high concentrations of non-deuterated solutes, a HX protocol referred to as the quench method is used. In this method, HX is initiated in the presence of non-deuterated solutes. At desired time intervals, aliquots of the HX reaction are withdrawn and the HX is quenched quickly. Prior to NMR analysis, the protein is separated from the non-deuterated solutes under the quenching conditions. It should be noted that the quench idea is not new since all "pulsed H/D" experiments as well as some other HX experiments have used this approach (Bai et al., 1994; Udgaonkar & Baldwin, 1988, 1990; Wagner & Wüthrich, 1982; Roder et al., 1985). However, the validity of the method has not been examined in detail. We demonstrate experimentally that the quench method gives HX rates identical to those obtained by the tandem method. Using the quench method, the effects of sucrose (a typical compatible osmolyte) on the internal structural fluctuations of RNase A are investigated. The effects of sucrose on the intrinsic chemical HX rates are also examined.

MATERIALS AND METHODS

Materials. Bovine pancreatic RNase A was obtained from Sigma Chemical Co. (type XII A) and ICN. The proteins were found to be electrophoretically pure and were used without further purification. D_2O (99.96% D) was from Cambridge Isotope Laboratories, and DCl (20% DCl in D_2O, 99% D), sucrose, and poly-DL-alanine (PDLA) were all from Sigma.

HX Protocols for the Tandem and Quench Methods. For the tandem method, the HX reaction is initiated by dissolving lyophilized protein into D_2O containing the desired additives (e.g., salt, buffer, and chemical shift standard) at a specified pH and temperature. Additives should be selected so that they do not interfere with protein resonances nor cause any signal dynamic range problems in the NMR measurements. Such constraints often require the use of fully deuterated forms of the additives. Once dissolved, the sample is ready for collecting NMR spectra as a function of time. The NMR acquisition parameters as well as data analysis should be kept the same for all NMR spectra. Consecutive data points are obtained by acquisition of a series of multidimensional NMR spectra one after the other (i.e., in tandem).

For the quench method, the HX reaction is initiated by dissolving protein in D_2O containing desired additives (e.g., salt, buffer, and chemical shift standard) at a specified pH and temperature. Aliquots of the reaction mixture are withdrawn at desired intervals, and the HX reaction is slowed or quenched, for example, by decreasing temperature, changing pH, adding a ligand, or any combination of these conditions. For cases in which additives used in the HX reaction interfere with acquisition or interpretation of NMR data, the additives may be separated from protein (e.g., by rapid gel filtration) after the quench and prior to NMR measurements. The protein samples should be kept frozen until acquisition of NMR data. To obtain reliable HX rate constants, it is essential to treat all the samples identically and to keep the NMR acquisition parameters and the data analysis the same for all samples.

Experimental Test of the Quench Method. The HX experiments of RNase A were carried out according to the two protocols described above. RNase A was lyophilized from aqueous solution at pH 4.9. The HX temperature (28.4 °C) and pH (pH* 4.9) were kept the same for the tandem and quench methods in order to make direct comparisons of the rate constants obtained by the two methods. The samples for the quench method were quenched quickly by freezing them in a bath of ethanol and dry ice, and the samples were kept at −20 °C until NMR measurement. The NMR acquisition and data analysis are described below.

NMR Data Acquisition and Analysis. The 1D ^1H and 2D absolute value $^1H-^1H$ COSY (Aue et al., 1976) spectra were obtained using a Varian 400 MHz NMR spectrometer. Both the proton and the decoupler frequencies were set on the water peak (4.78 ppm). Water presaturation was applied during the 3.5 s recycle delay by continuous low-power irradiation. For each COSY spectrum, 2048 data points were collected along the t_2 domain, each consisting of 16 summed scans, and 256 data points were collected along the t_1 domain. The spectral width was 4800 Hz, and the temperature at 30 °C. The acquisition time for each COSY spectrum was about four hours. Prior to Fourier transformation, COSY data in both dimensions were weighted by unshifted sine-bell functions and zero-filled once. The amide proton peaks were then assigned according to the published proton chemical shifts of RNase A (Rico et al., 1989; Robertson et al., 1989). The selected amide proton peak intensities were analyzed using the Varian software, which gives the position, amplitude and volume of each peak. For each $NH/C_\alpha H$ cross peak, the ratio of volume or amplitude was calculated relative to that of the Tyr 25 ring proton cross peak. The ratio as a function of HX time was fitted to a first-order exponential function plus a constant due to the threshold setting used in the program. Since the threshold needs to be set above the NMR base line, the constant can have negative values.

HX of RNase A in the Presence and Absence of 1 M Sucrose at 35 °C. The HX experiments were carried out using the quench protocol described above. Prior to the HX reaction, RNase A was lyophilized from aqueous solution at pH 6.5 and sucrose was lyophilized twice from D_2O solutions at pH* 6.5. HX reaction was initiated by dissolving the lyophilized protein into D_2O (±1 M sucrose). At different HX times, ranging from several minutes to about a week, aliquots (~0.6 mL) of the HX reaction were withdrawn and HX was quenched by dropping the pH* to 3.5 with DCl. Samples were quickly frozen and stored at −20 °C until analysis by NMR. For those samples containing 1 M sucrose, the sucrose was separated from protein using a small G-25 HiTrap column (Pharmacia) prior to NMR measurements. The separation took only a minute or so and was complete, with the protein being diluted less than 2-fold. The final protein concentration for all NMR measurements was about 2 mM.

The procedures for the HX experiments at pH* 7.4 (±1 M sucrose) were the same as those of the HX experiments carried out at pH* 6.5, except that the pH* was increased to 7.4 and 0.1% NaN_3 was included in the HX reactions to prevent bacterial growth during the HX periods (35 days in the absence and 46 days in the presence of sucrose). To monitor possible decomposition of sucrose, the sucrose fractions obtained from the HiTrap column and a control sample, containing only sucrose in D_2O, were checked by 1D proton NMR as a function of incubation time.

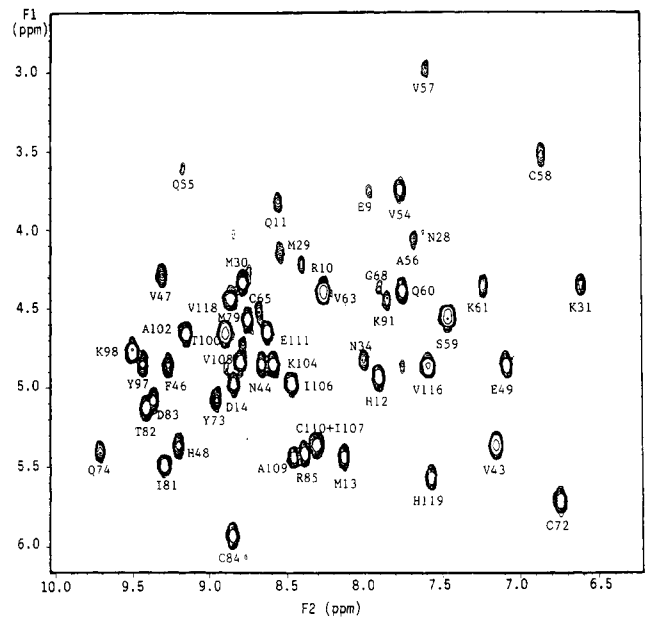

FIGURE 1: $^1H-^1H$ COSY spectrum of RNase A amide proton region at pH* 3.5, 30 °C. The protein sample was exchanged with solvent D_2O for 3 minutes at pH* 6.5, 35 °C, and then quenched with DCl. The resonances were assigned according to the published chemical shifts for RNase A (Robertson et al., 1989; Rico et al., 1989).

HX Rate Measurements of PDLA in the Presence and Absence of 1 M Sucrose. The H/H exchange rate constants for PDLA (±1 M sucrose) were measured at 35 °C using saturation transfer (Dempsey, 1986; Forsen & Hoffman, 1963; O'Neil & Sykes, 1989). Data were acquired on a Varian 500 MHz NMR spectrometer located in the College of Medicine NMR Facility at the University of Iowa. The PDLA samples contained about 3.5 mg of polypeptide/mL and 50 mM sodium phosphate (±1 M sucrose) in 10% D_2O/90% H_2O. The NH peak intensity reached a steady-state level after the water resonance had been preirradiated for 0.5 s. A solvent preirradiation time of 1.5 s was used in all experiments, and the total recycle delay was 5.8 s. A 2 Hz line-broadening was applied, and the FID was zero-filled once prior to Fourier transformation. After base line correction, the NH peak intensity was normalized to that of the nonexchanging methyl protons. The normalized intensity (I) was used to calculate the H/H exchange rate constant (k_{ex}) by eq 1. The T_1 (measured by the inversion-recovery

$$I/I_0 = 1/(1 + k_{ex}T_1) \quad (1)$$

method) and I_0 values in eq 1 were measured under conditions where the HX rate is slow, pH 3−3.5, 35.0 °C.

D/H exchange rate constants for PDLA (±1 M sucrose) at 35.0 °C were measured spectrophotometrically (Englander et al., 1979). Aliquots (15 μL) of PDLA (36 mg/mL in D_2O) were diluted into 2.5 mL aqueous solutions (±1 M sucrose, 50 mM NaCl, and 10 mM NaH_2PO_4) at specified pH values and 35.0 °C. The absorbance change at 220 nm was followed as a function of time using an Olis-14 UV spectrophotometer. D/H exchange rate constants were obtained by fitting the kinetic curves to a single-exponential equation plus a constant, and the pH of the reaction solutions was measured after each kinetic experiment.

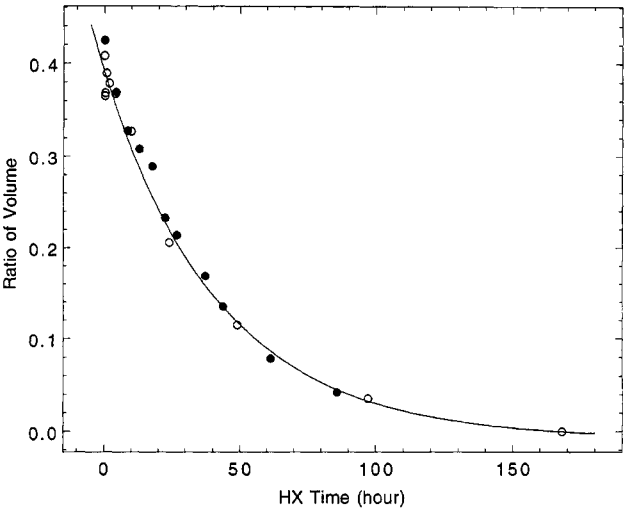

FIGURE 2: HX kinetics for Ser 59 amide proton of RNaseA at pH* 4.9, 28.4 °C, by the tandem method (●) and the quench method (○). The ratio of volume is the ratio of the volume of Ser 59 to that of the nonexchanging Tyr 25 ring protons. The solid line is a first-order fit to the quench data, which gives a HX rate constant of (2.35 ± 0.30) × 10^{-2} h^{-1}. A first-order fit to the tandem data provides a HX rate constant of (2.31 ± 0.25) × 10^{-2} h^{-1}.

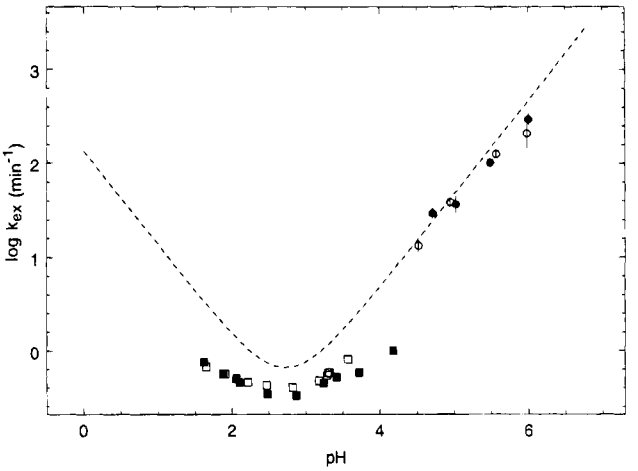

FIGURE 3: H/H (represented by circles) and D/H (represented by squares) exchange rate constants of PDLA as a function of pH at 35.0 °C. The filled and open symbols represent data measured in the presence or absence of 1 M sucrose, respectively. The fitting errors in D/H rate constants are within the sizes of symbols. The dashed line is the predicted exchange rate constants for PDLA (in the absence of sucrose) using the data of Bai et al. (1993).

RESULTS

COSY Spectrum of RNase A. Figure 1 is a representative COSY spectrum of the RNase A amide proton region obtained for a quenched sample that had been exchanged with D_2O for 3 min. The resonances were assigned according to the published chemical shifts of RNase A (Robertson et al., 1989; Rico et al., 1989). As shown in Figure 1, most of the amide protons are well resolved, making it possible to evaluate HX rate constants for individual amide protons directly.

HX Rate Constants of RNase A Obtained by the Tandem and Quench Methods. To examine the validity of the quench method, the HX rate constants of RNase A amide protons at 28.4 °C, pH* 4.9, were measured using both the tandem and quench protocols as described. Figure 2 shows, as an example, the exchange kinetics for Ser 59 using the two

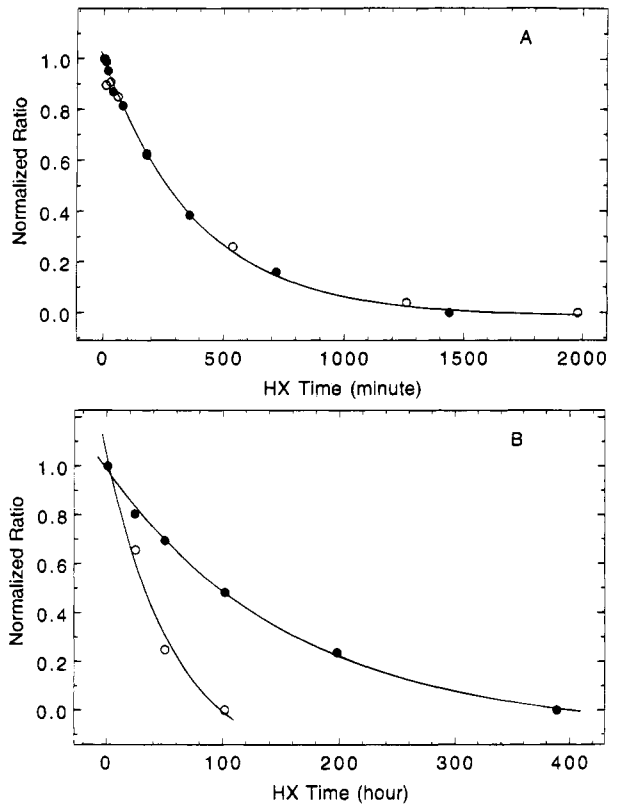

FIGURE 4: Representative HX kinetics of RNase A amide protons in the presence (●) or absence (○) of 1 M sucrose at 35.0 °C. (A) The HX kinetics of Ser 59 amide proton at pH* 6.5. (B) The HX kinetics of His 119 amide proton at pH* 7.4. The ratio of peak amplitude or volume was normalized to the start of HX and was fitted to a first-order exponential plus a constant. The HX rate constants obtained from such fits in the absence or presence of sucrose are $(2.44 \pm 0.28) \times 10^{-3}$ min^{-1} and $(2.58 \pm 0.19) \times 10^{-3}$ min^{-1} (solid line in A) for Ser 59 and $(2.83 \pm 0.50) \times 10^{-4}$ min^{-1} and $(1.04 \pm 0.15) \times 10^{-4}$ min^{-1} for H119.

methods. The quench method gives an HX rate constant of $(2.35 \pm 0.3) \times 10^{-2}$ h^{-1}, overlapping with the rate constant of $(2.31 \pm 0.25) \times 10^{-2}$ h^{-1} obtained by the tandem method. Within experimental error, the rate constants obtained by the two methods are essentially identical for all measured amide protons.

Effects of 1 M Sucrose on the Chemical HX Rate Constants of PDLA at 35.0 °C. The chemical HX rate constants were measured in the presence and absence of 1 M sucrose using PDLA, a typical model compound used in chemical HX rate calibration (Bai et al., 1993; Molday et al., 1972). In Figure 3, H/H exchange rate constants were determined at higher pH values using the saturation−transfer method, while D/H exchange rate constants were obtained at lower pH values spectrophotometrically. The D/H exchange rate constants were smaller than the predicted H/D exchange rate constants (Bai et al., 1993), which may be due to the isotopic effect and the rapid loss of signal during the mixing time at 35 °C. Over all of the pH values examined, the presence of 1 M sucrose has no significant effect on either the H/H or the D/H exchange rate constants of PDLA.

HX Rate Constants of RNase A in the Presence and Absence of 1 M Sucrose at 35.0 °C, pH 6.5.* To investigate the effects of sucrose on HX of RNase A, HX experiments were first carried out at 35.0 °C, pH* 6.5, for about 1 week. Representative kinetic curves are shown in Figure 4A, and HX data are summarized in Table 1.

The observed HX rates for RNase A in the absence of sucrose are slowed to varying extents relative to rates obtained with the unstructured peptides (Bai et al., 1993), with some too slow to be monitored within the experimental time window. The protection factors, defined as the ratio of the chemical HX rate constant to the observed HX rate constant of a specific amide proton (Bai et al., 1993), are shown in Figure 5A. The amide protons that exchange too slowly to be evaluated are arbitrarily given a value of 10^9 in Figure 5A (open circles) and are hereafter referred to as slow-exchanging amide protons. For those amide protons whose HX rate constants are measurable within the experimental time window, the protection factors vary considerably, covering a range of about 4 orders of magnitude. These amide protons are referred to as intermediate-exchanging amide protons.

A comparison of the HX rates for the intermediate-exchanging amide protons in the presence and absence of sucrose is shown in Figure 6. The HX rate constants of the intermediate-exchanging amide protons are essentially identical in the presence and absence of sucrose, differing by a factor of less than 2 for each amide site. These differences are not believed to be statistically significant.

HX Rate Constants of RNase A in the Presence and Absence of 1 M Sucrose at 35.0 °C, pH 7.4.* To measure the HX rate constants of the slow-exchanging amide protons, HX was also carried out at a higher pH* (pH* 7.4), and the observation time window was much longer (up to 46 days). No sucrose or protein decomposition was detected by NMR during this time. Figure 4B shows representative kinetic curves of amide proton His 119. The resulting HX rate constants in the presence and absence of 1 M sucrose are listed in Table 1 and compared in Figure 7.

In Figure 7, the filled circles represent those amide protons whose HX rates are also measured in the pH* 6.5 experiments (filled circles in Figures 5A and 6), and the open circles represent those amide protons that exchange too slowly to be measured in the pH* 6.5 experiments (open circles in Figure 5A). Sucrose does not affect the HX kinetics of the intermediate-exchanging amide protons at pH* 6.5 (Figure 6) nor is there much of an effect at pH* 7.4. However, as the amide proton HX rate becomes slower, the data deviate uniformly and significantly from the diagonal. This shows that sucrose reduces HX rates of the slow-exchanging amide protons.

The protection factors of amide protons (in the absence of sucrose) along the protein backbone at pH* 7.4 are plotted in Figure 5B. The open circles signify those amide protons that are immeasurably slow in the pH* 6.5 experiment, and most of them have about the same magnitude of protection factors relative to one another, in the range 10^7-10^8. By contrast, the filled circles in Figure 5B represent amide protons whose rates are measured in both the pH* 6.5 and 7.4 experiments, and most of them have smaller protection factors, in the range of 10^5-10^7.

DISCUSSION

Combined with advances of modern NMR techniques, HX kinetics can be resolved at individual exchange sites, and it is used widely to investigate protein conformations, internal dynamics, and stability. For the HX experiments carried out using the tandem method, the time-averaged NMR signal

Table 1: HX Rate Constants (in min^{-1}) of RNase A at 35.0 °C, pH* 6.5 or 7.4, ±1 M Sucrose

	pH* 6.5				pH* 7.4			
amide proton	$k_{(chem)}$[a]	$k_{(-suc)}$	PF[b]	$k_{(+suc)}$	$k_{(chem)}$[a]	$k_{(-suc)}$	PF[b]	$k_{(+suc)}$
R10	3.14×10^{2}	1.81×10^{-3}	1.74×10^{5}	2.64×10^{-3}	2.23×10^{3}	fast		fast
Q11	7.04×10^{2}	4.08×10^{-5}	1.73×10^{7}	5.93×10^{-5}	4.98×10^{3}	4.12×10^{-3}	1.21×10^{6}	1.51×10^{-3}
H12	3.70×10^{3}	slow		slow	2.62×10^{4}	2.33×10^{-3}	1.12×10^{7}	1.24×10^{-3}
M13	2.44×10^{3}	slow		slow	1.73×10^{4}	1.48×10^{-3}	1.17×10^{7}	
D14	2.39×10^{2}	1.29×10^{-3}	1.85×10^{5}	1.44×10^{-3}	1.69×10^{3}	2.05×10^{-2}	8.24×10^{4}	1.06×10^{-2}
M29	5.72×10^{2}	7.21×10^{-4}	7.94×10^{5}	7.20×10^{-4}	4.05×10^{3}	fast		fast
M30	4.65×10^{2}	1.92×10^{-2}	2.42×10^{4}	1.44×10^{-2}	3.29×10^{3}	fast		fast
K31	4.34×10^{2}	1.24×10^{-2}	3.50×10^{4}	2.17×10^{-2}	3.07×10^{3}	fast		fast
N34	1.90×10^{3}	8.07×10^{-2}	2.35×10^{4}	6.00×10^{-2}	1.34×10^{4}	fast		fast
V43	4.24×10^{1}	9.29×10^{-3}	4.57×10^{3}	1.21×10^{-2}	3.00×10^{2}	fast		fast
N44	8.28×10^{2}	1.68×10^{-3}	4.93×10^{5}	1.39×10^{-3}	5.86×10^{3}	fast		fast
F46	3.37×10^{2}	slow		slow	2.39×10^{3}	4.72×10^{-5}	5.06×10^{7}	1.68×10^{-5}
V47	8.47×10^{1}	slow		slow	5.99×10^{2}	3.32×10^{-5}	1.81×10^{7}	1.88×10^{-5}
H48	1.69×10^{3}	2.28×10^{-4}	7.41×10^{6}	1.38×10^{-4}	1.20×10^{4}	3.17×10^{-4}	3.77×10^{7}	2.56×10^{-4}
E49	7.72×10^{2}	1.74×10^{-3}	4.44×10^{5}	1.45×10^{-3}	5.47×10^{3}	3.01×10^{-3}	1.82×10^{6}	2.77×10^{-3}
V54	4.87×10^{1}	slow		slow	3.45×10^{2}	1.92×10^{-4}	1.80×10^{6}	1.03×10^{-4}
Q55	3.07×10^{2}	slow		slow	2.18×10^{3}			
A56	5.86×10^{2}	2.59×10^{-4}	2.26×10^{6}	3.55×10^{-4}	4.15×10^{3}	3.22×10^{-3}	1.29×10^{6}	5.07×10^{-3}
V57	7.37×10^{1}	slow		slow	5.22×10^{2}			
C58	9.50×10^{2}	slow		slow	6.72×10^{3}	1.24×10^{-4}	5.42×10^{7}	5.03×10^{-5}
S59	2.50×10^{3}	2.44×10^{-3}	1.02×10^{6}	2.58×10^{-3}	1.77×10^{4}	fast		fast
Q60	8.47×10^{2}	8.53×10^{-4}	9.93×10^{5}	9.01×10^{-4}	5.99×10^{3}	fast		fast
K61	5.34×10^{2}	1.78×10^{-3}	3.00×10^{5}	1.50×10^{-3}	3.78×10^{3}	fast		fast
V63	1.54×10^{2}	slow		slow	1.09×10^{3}	4.10×10^{-4}	2.66×10^{6}	2.35×10^{-4}
C65	1.31×10^{3}	3.74×10^{-2}	3.51×10^{4}	3.04×10^{-2}	9.28×10^{3}	fast		fast
C72	2.74×10^{3}	9.57×10^{-5}	2.86×10^{7}	1.62×10^{-4}	1.94×10^{4}	9.53×10^{-3}	2.03×10^{6}	8.79×10^{-3}
Y73	5.73×10^{2}	slow		slow	4.05×10^{3}	4.98×10^{-5}	8.13×10^{7}	1.52×10^{-5}
Q74	4.76×10^{2}	slow		slow	3.37×10^{3}	4.33×10^{-5}	7.78×10^{7}	1.18×10^{-5}
M79	5.73×10^{2}	slow		slow	4.05×10^{3}	6.97×10^{-5}	5.82×10^{7}	1.42×10^{-5}
I81	1.37×10^{2}	slow		slow	9.72×10^{2}	3.77×10^{-5}	2.58×10^{7}	9.13×10^{-6}
T82	1.85×10^{2}	slow		slow	1.31×10^{3}	3.62×10^{-5}	3.63×10^{7}	6.45×10^{-6}
D83	2.94×10^{2}	2.32×10^{-3}	1.27×10^{5}	slow	2.08×10^{3}	fast		fast
C84	8.66×10^{2}	5.98×10^{-5}	1.45×10^{7}	6.01×10^{-5}	6132.3	8.26×10^{-4}	7.42×10^{6}	5.71×10^{-4}
K91	6.73×10^{2}	7.8×10^{-2}	8.62×10^{3}	5.76×10^{-2}	4.76×10^{3}	fast		fast
Y97	1.99×10^{2}	1.18×10^{-2}	1.68×10^{4}	1.43×10^{-2}	1.40×10^{3}	fast		fast
K98	3.78×10^{2}	8.51×10^{-5}	4.44×10^{6}	6.91×10^{-5}	2.68×10^{3}	9.53×10^{-3}	2.81×10^{5}	4.53×10^{-3}
T100	4.99×10^{2}	2.43×10^{-4}	2.05×10^{6}	2.63×10^{-4}	3.53×10^{3}	8.57×10^{-3}	4.12×10^{5}	7.30×10^{-3}
A102	5.86×10^{2}	1.36×10^{-4}	4.31×10^{6}	1.44×10^{-4}	4.15×10^{3}	7.99×10^{-3}	5.19×10^{5}	3.20×10^{3}
K104	7.04×10^{2}	slow		slow	4.98×10^{3}	4.60×10^{-4}	1.08×10^{7}	2.25×10^{-4}
I106	4.65×10^{2}	slow		slow	3.29×10^{3}	2.87×10^{-5}	1.15×10^{8}	1.64×10^{-5}
V108	4.34×10^{1}	slow		slow	3.07×10^{2}	1.90×10^{-5}	1.60×10^{7}	7.10×10^{-6}
A109	2.68×10^{2}	slow		slow	1.90×10^{3}	2.45×10^{-5}	7.7×10^{7}	1.02×10^{-5}
E111	3.29×10^{2}	1.93×10^{-4}	1.71×10^{6}	2.58×10^{-4}	2.33×10^{3}	8.65×10^{-3}	2.70×10^{5}	7.49×10^{-3}
V116	8.28×10^{1}	slow		slow	5.86×10^{2}	6.17×10^{-5}	9.50×10^{6}	2.47×10^{-5}
V118	4.24×10^{1}	slow		slow	3.00×10^{2}	6.23×10^{-5}	4.82×10^{6}	1.73×10^{-5}
H119	1.69×10^{3}	slow		slow	1.20×10^{4}	2.83×10^{-4}	4.22×10^{7}	1.04×10^{-4}

[a] $k_{(chem)}$ is the predicted HX rate constant at 35 °C, pH* 6.5 or 7.4 (Bai et al., 1993). [b] PF stands for protection factor, which is the ratio $k_{(chem)}/k_{(-suc)}$. Rate constants indicated as "slow" are estimated to be smaller than 10^{-5} min^{-1}, while those marked as "fast" are estimated to be larger than 10^{-2} min^{-1}.

intensity of amide proton i (A_i) in the spectrum collected at time t_{HX} is (Wagner & Wüthrich, 1982)

$$\bar{A}_i(t_{HX}) = R_1 A_0 \exp(-k_{HX} t_{HX}) \quad (2)$$

$$\text{with} \quad R_1 = \left[\frac{1 - \exp(-k_{HX} T_{NMR})}{k_{HX} T_{NMR}}\right] \quad (3)$$

where k_{HX} is the HX rate constant, T_{NMR} is the NMR acquisition time, and A_0 is the initial NMR intensity at time zero. For an amide proton exchanging with rate constant k_{HX}, R_1 is a constant when the NMR acquisition time is kept the same in each NMR spectrum. It represents the decrease in signal intensity due to HX during NMR data acquisition. The nonlinear least-squares fitting of peak intensity with HX time (eq 2) provides the HX rate constant k_{HX} as a fitting parameter. However, fast HX rate constants measured by the tandem method are limited by the NMR acquisition time, T_{NMR}.

Here, we develop and test a HX quench method that has advantages over the tandem method. The time-averaged NMR signal intensity of proton i in a HX sample quenched at t_{HX} is (Wagner & Wüthrich, 1982)

$$\bar{A}_i(t_{HX}) = R_2 A_0 \exp(-k_{HX} t_{HX}) \quad (4)$$

$$\text{with} \quad R_2 = \left[\frac{1 - \exp(-k_{NMR} T_{NMR})}{k_{NMR} T_{NMR}}\right] \quad (5)$$

where k_{NMR} is the HX rate constant under NMR data acquisition conditions. According to eq 4, R_2 will be a constant provided all samples are treated the same in terms of quenching and NMR data acquisition. Consequently, nonlinear least-squares fitting of the signal intensity with HX time will provide the HX rate constant (k_{HX}) without any complications from k_{NMR}. Here, R_2 represents the decreased signal intensity with a value between 0 and 1. However, in

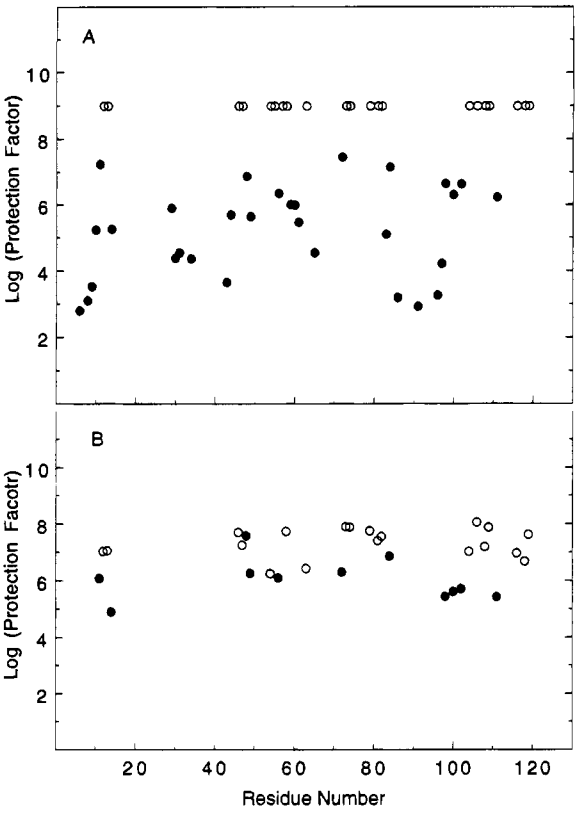

FIGURE 5: Protection factors of RNase A amide protons at pH* 6.5 (A) and pH* 7.4 (B) in the absence of sucrose (35.0) °C. The open circles are slow-exchanging amide protons, and the closed circles are intermediate-exchanging amide protons, as defined in the text. The errors in protection factors are generally within the same sizes of symbols.

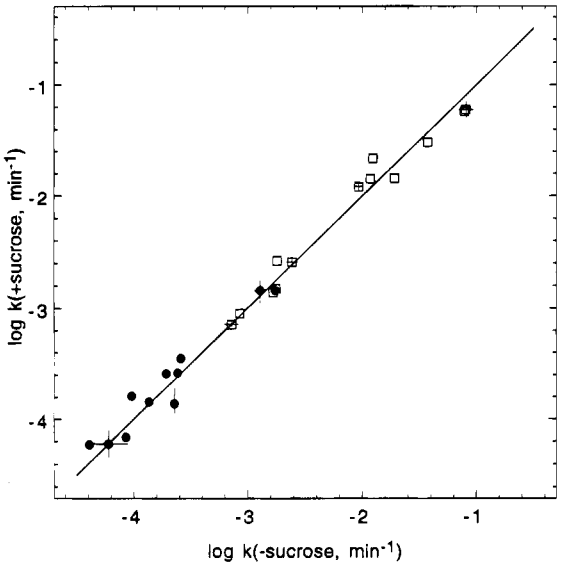

FIGURE 6: Comparison of HX rate constants (k) in the presence or absence of 1 M sucrose at pH* 6.5, 35 °C. The filled circles represent the amide protons that were measured in both the pH* 6.5 and 7.4 experiments (filled circles in Figure 7), while the open squares represent the amide protons that were measured only at pH* 6.5. The error bars in the HX rate constants of some protons are given as being representative of the x and y errors in that region of the log−log plot.

contrast to R_1 (eq 3), R_2 is independent of the HX rate constant (k_{HX}) to be measured, and its value may be maintained close to 1 by choosing proper quench conditions and T_{NMR}. When the NMR samples are efficiently quenched,

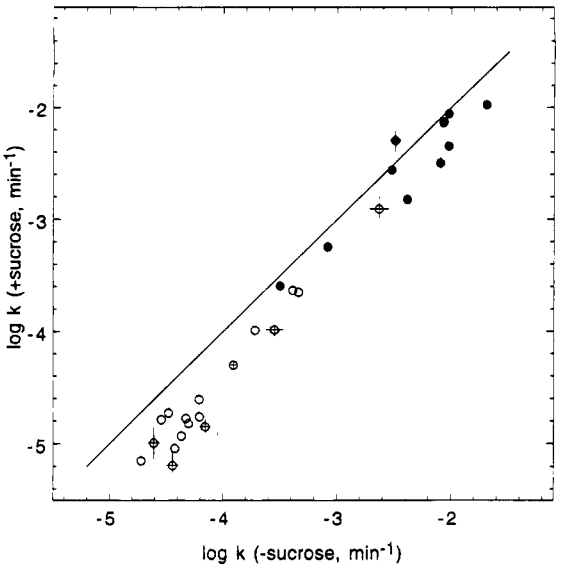

FIGURE 7: Comparison of HX rate constants (k) in the presence or absence of 1 M sucrose at pH* 7.4, 35 °C. The filled circles represent the amide protons that were measured in both the pH* 6.5 and 7.4 experiments (filled circles in Figure 6), while the open circles represent the slow-exchanging amide protons that were measured only at pH* 7.4. The error bars in the HX rate constants of some protons are given as being representative of the x and y errors in that region of the log−log plot.

the fastest HX rate constant that can be measured by the quench method will depend only on how fast the HX reaction is sampled and quenched.

As shown by these equations, the quench method should yield rate constants identical to those obtained with the tandem method. Under the experimental conditions used, the HX rate constants from the tandem and quench methods are the same within experimental error (Figure 2). While the quench method requires more protein, it has several advantages over the tandem method. For example, the quench method can be used to resolve fast HX rates. Moreover, it allows one to study HX over a much wider range of experimental conditions, including the presence of non-deuterated additives as well as larger pH and temperature ranges. In addition, it provides more flexibility in scheduling NMR time since the NMR samples can be stored under quench conditions for later NMR measurements.

Using the quench method, HX from RNase A in the absence of sucrose was measured at pH* 6.5 and pH* 7.4 to characterize those amide protons that undergo HX at intermediate and slow rates. Inspection of the RNase A structure (Wlodawer et al., 1988; Santoro et al., 1993) reveals that most of the protected amide protons are H-bonded, with few exceptions. All protected amide protons are located either in β-sheets or in α-helices, indicating reduced structural fluctuations in these regions, particularly in the two β-sheets. RNase A refolding experiments identified a group of amide protons that are highly protected during protein refolding (V47, H48, V54, V63, C72, Y73, I81, C84, K98, I106, V108, V116, V118, H119); (Udgaonkar & Baldwin, 1990). These amides are found to be a subset of highly protected protons in our HX studies (Table 1). This is consistent with the proposal by Kim and Woodward (1993) that the protein folding core is within the slow-exchange core.

In terms of the HX mechanisms, our RNase A HX data fit very well with the two-process model, which was first

proposed by Woodward and Hilton (1980) and observed recently in many systems (Bai et al., 1994; Kim & Woodward, 1993; Mayo & Baldwin, 1993; Qian et al., 1994). In the two-process model, the HX for a labile proton is proposed to occur from the native state ensemble and from the unfolded state ensemble. Under certain experimental conditions, exchange by one process may dominate over exchange by the other process, and the dominant process may differ from proton to proton.

For those intermediate-exchanging amide protons identified in the pH* 6.5 HX experiments, the HX occurs mainly from the native state ensemble of the protein based on the following observations: the protection factors cover a range of more than 4 orders of magnitude; many amide protons have protection factors that are quite different from their nearest neighbors (Figure 5A); the HX rate constants for several of these amide protons are measured in both pH* 7.4 and pH* 6.5 experiments, and the ratio of the rate constant at pH* 7.4 to that at pH* 6.5 varies from 1 to 100 for different amide protons (Table 1). This latter result is very different from what is expected from unstructured polypeptides. PDLA, for example, has a rate constant ratio of about 8 over this pH range. In contrast to those intermediate-exchanging amide protons, the slow-exchanging amide protons identified in the pH* 7.4 experiments have a narrower range of protection factors relative to each other (open circles in Figure 5B). This indicates that these protons have similar structural fluctuation modes that lead to exchange, namely, HX occurs mainly from the unfolded state ensemble of the protein. Numerous studies have been carried out to investigate the temperature- and denaturant-dependence of amide proton exchanging rates, and the results also indicate that under native conditions, HX occurs mainly from the native state for the relatively fast-exchanging amide protons and mainly from the unfolded state for the slow-exchanging amide protons (Akasaka et al., 1985; Bai et al., 1994; Kim & Woodward, 1993; Mayo & Baldwin, 1993; Qian et al., 1994; Woodward et al., 1982; L. Swint-Kruse and A. D. Robertson, unpublished results).

HX data have been used to evaluate protein thermodynamic quantities (Berger & Linderstrøm-Lang, 1957; Hvidt & Nielsen, 1966; Wagner & Wüthrich, 1979).

$$\text{native-state} \overset{K_{op}}{\longleftrightarrow} \text{open-state} \overset{\underset{k_{ch}}{HX}}{\longrightarrow}$$

$$\text{open-state*} \overset{K_{op}}{\longleftrightarrow} \text{native-state*}$$

$$k_{obs} = K_{op}k_{ch} \qquad (6)$$

Under EX2 conditions, the observed HX rate constant (k_{obs}) is the product of k_{ch} (the intrinsic chemical HX rate constant) and K_{op} (the equilibrium constant of the native- and open-states of protein). In the case where HX is occurring from the denatured state, K_{op} represents the denaturation equilibrium constant between native and denatured protein in aqueous solution, making it possible to estimate the unfolding free energy change ($\Delta G°_{N-U} = -RT \ln K_{op}$). Such a calculation for the slow-exchanging amide protons of RNase A gives a $\Delta G°_{N-U}$ that is about 2−3 kcal/mol more stable than expected from denaturation experiments (Yao & Bolen, 1995). Similar discrepancies have also been reported for cytochrome *c* (Bai et al., 1994) and BPTI (Roder, 1989) as well as RNase A (Mayo & Baldwin, 1993) and ovomucoid third domain (L. Swint-Kruse and A. D. Robertson, unpublished results). The origins of disagreement between HX data and denaturation data are not clear. Mayo and Baldwin (1993) suggest that it may arise from a substantial difference between the rates of exchange in an unfolding intermediate and in an unstructured peptide, while Bai et al. (1994) suggest that proline isomerization may contribute significantly to the difference. The use of D_2O in the HX studies may also contribute to the discrepancy since D_2O is known to cause an increase in the thermal transition temperature of protein compared to that in H_2O. Another possible explanation is that HX occurs by the EX1 mechanism (Bai et al., 1994; L. Swint-Kruse and A. D. Robertson, unpublished results). However, the possibility we favor comes from the likelihood that the denatured state in aqueous media and strong denaturing media are thermodynamically different. The unfolding free energy change obtained from the linear extrapolation, for a protein like RNase A, represents the free energy difference between native and extensively unfolded protein *projected* to the limit of zero denaturant concentration (Yao & Bolen, 1995). The unfolded ensemble from this equilibrium is unlikely to be thermodynamically equivalent to the denatured ensemble which actually occurs in the absence of denaturant, since one originates from a "good" solvent (urea or guanidine hydrochloride) giving an extensively unfolded ensemble, while the other conforms to the constraints of a poor solvent (water) to give a compact denatured state (Mayr & Schmid, 1993; Santoro & Bolen, 1992; Dill & Shortle, 1991). *A priori*, there is no reason to expect the free energy change estimated from the two techniques to be the same since they represent reactions with different participants.

The presence of compact unfolded states of protein under protein native state conditions is also consistent with our protection factor data of the slow-exchanging amide protons (Figure 5B). In principle, the amide protons of a fully unfolded protein should have identical protection factors. However, we observe that the protection factors for the slow-exchanging amide protons cover a range of about 100-fold, suggesting the presence of residual structure in the (compact) denatured states.

Comparison of HX rate constants with and without 1 M sucrose shows that sucrose does not affect the HX kinetics of the intermediate-exchanging amide protons (Figure 6); it only reduces the HX rates of those slow-exchanging amide protons (Figure 7). Similar observations were observed with H/T exchange experiments on myoglobin and lysozyme in the presence of glycerol, another compatible osmolyte (Calhoun & Englander, 1985; Gregory, 1988; Knox & Rosenberg, 1980). Though these experiments could not observe H/T exchange from individual amides, they show that only the rates of the slowest-exchanging protons are changed (decreased) by the presence of glycerol.

Thermodynamic measurements of the effects of sucrose and glycerol on protein stability provides a framework for discussing dynamic and thermodynamic issues. Equilibrium dialysis and transfer free energy measurements show that protein unfolding free energy changes in water and osmolyte solutions are related as shown in Scheme 1 (Gekko & Timasheff, 1981a,b; Lee & Timasheff, 1981; Timasheff, 1993; Liu & Bolen, 1995). Here we see that the transfer free energy of the native protein from water to osmolyte is

Scheme 1

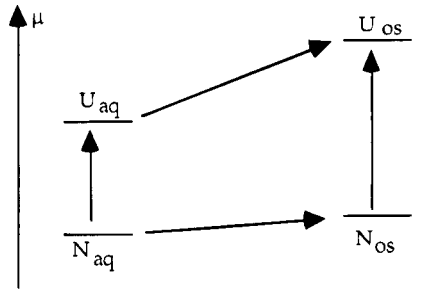

slightly unfavorable while the free energy of transfer of unfolded protein from water to osmolyte is very unfavorable. The reason an osmolyte stabilizes proteins against denaturation is not because of a stabilizing effect on the native state. Quite the contrary, it is due to the very large destabilization of the denatured state in the presence of osmolyte, causing a larger free energy difference between the native and the unfolded states in the presence of osmolyte. The destabilization of the native and denatured states have their origins in the unfavorable interactions of the peptide backbone with osmolyte (Liu & Bolen, 1995). The denatured state is more destabilized than the native state due to the greater degree of backbone exposure in this state.

The effects of sucrose on the internal dynamics of RNase A fit very well with both the thermodynamic measurements (Scheme 1) and the two-process model discussed earlier. Sucrose has no affect on the chemical HX rates (Figure 2), and if exchange occurs by the EX2 mechanism, any effects that sucrose has on the HX kinetics of RNase A should be due to its effects on the K_{op} of the protein (equation 6). For those slow-exchanging amide protons, the exchange mechanism requires structural fluctuations with larger surface exposure, involving unfolding of the protein. That is, the exchange of these amide protons occurs mainly from the unfolded state ensemble of the protein. These amide protons are also the only ones that are affected by sucrose. The smaller rate constants in sucrose (as compared to those in water) for these amide protons are observed and expected on the basis of the following reasoning: (1) The presence of sucrose opposes the structural fluctuations leading to unfolded protein because of the unfavorable thermodynamic interactions between protein surface and sucrose (Lee & Timasheff, 1981; Timasheff, 1993; Liu & Bolen, 1995); (2) This unfavorable interaction will also lead to a more compact unfolded state ensemble in the presence of sucrose. The effect of 1 is a decrease in the HX rate by decreasing the population of unfolded protein, while the effect of 2 is slowed HX through the formation of compact structure.

For the intermediate-exchanging amide protons, HX occurs mainly from the native state ensemble of the protein. The native protein has minimal surface contact with sucrose, and the chemical potential of the native protein in sucrose is only slightly increased from that in water (Scheme 1). As a result, the native protein conformations and population are not perturbed significantly by sucrose under our HX conditions. Consequently, the internal dynamics of the intermediate-exchanging amide protons are not affected by the presence of sucrose, as observed by HX. This means that the microstates which compose the native state ensemble, and from which the amide exchange takes place, are populated to essentially the same extent in 1 M sucrose and in water. Because the microstates of the native state ensemble are believed to be important in protein function, the fact that they are relatively unchanged in the presence of sucrose provides a basis for understanding how sucrose affects protein stability without affecting biological activity. That is, sucrose does not interfere significantly with the character and behavior of the native ensemble, it stabilizes the protein mainly by affecting the free energy and, therefore, the population of the denatured state ensemble. We propose that the above mechanism will hold for the effects of other compatible osmolytes on the interrelationships between protein stability, function and internal dynamics.

ACKNOWLEDGMENT

We thank Drs. John Shriver and Clare Woodward for their discussions on this work and comments on the manuscript.

REFERENCES

Akasaka, K., Inoue, T., Hatano, H., & Woodward, C. K. (1985) *Biochemistry 24*, 2973−2979.
Aue, W. P., Bartholdi, E., & Ernst, R. R. (1976) *J. Chem. Phys. 64*, 2229−2246.
Bagnasco, S., Balaban, R., Fales, H. M., Yang, Y.-M., & Burg, M. (1986) *J. Biol. Chem. 261*, 5872−5877.
Bai, Y., Milne, J. S., Mayne, L., & Englander, S. W. (1993) *Proteins 17*, 75−86.
Bai, Y., Milne, J. S., Mayne, L., & Englander, S. W. (1994) *Proteins 20*, 4−14.
Berger, A., & Linderstrøm-Lang, K. (1957) *Arch. Biochem. Biophys. 69*, 106−118.
Calhoun, D. B., & Englander, S. W. (1985) *Biochemistry 24*, 2095−2100.
Dempsey, C. E. (1986) *Biochemistry 25*, 3904−3911.
Dill, K. A., & Shortle, D. (1991) *Annu. Rev. Biochem. 60*, 795−825.
Englander, J. J., Calhoun, D. B., & Englander, S. W. (1979) *Anal. Biochem. 92*, 517−524.
Englander, S. W., & Kallenbach, N. R. (1984) *Q. Rev. Biophys. 16*, 521−655.
Forsen, S., & Hoffman, R. A. (1963) *J. Chem. Phys. 39*, 2892−2901.
Garcia-Perez, A., & Burg, M. B. (1990) *Hypertension 16*, 595−602.
Gekko, K., & Timasheff, S. N. (1981a) *Biochemistry 20*, 4667−4676.
Gekko, K., & Timasheff, S. N. (1981b) *Biochemistry 20*, 4677−4686.
Gregory, R. B. (1988) *Biopolymers 27*, 1699−1709.
Hvidt, A., & Nielsen, S. O. (1966) *Adv. Protein Chem. 21*, 287−386.
Kim, K.-S., & Woodward, C. K. (1993) *Biochemistry 32*, 9606−9613.
Kim, K.-S., Fuchs, J. A., & Woodward, C. K. (1993) *Biochemistry 32*, 9600−9608.
Knox, D. G., & Rosenberg, A. (1980) *Biopolymers 19*, 1049−1068.
Lee, J. C., & Timasheff, S. N. (1981) *J. Biol. Chem. 256*, 7193−7201.
Liu, Y., & Bolen, D. W. (1995) *Biochemistry 34*, 12884−12891.
Mayo, S. L., & Baldwin, R. L. (1993) *Science 262*, 873−876.
Mayr, L. M., & Schmid, F. X. (1993) *Biochemistry 32*, 7994−7998.
Molday, R. S., Englander, S. W., & Kallen, R. G. (1972) *Biochemistry 11*, 150−158.
O'Neil, J. D. J., & Sykes, B. D. (1989) *Biochemistry 28*, 699−707.
Qian, H., Mayo, S. L., & Morton, A. (1994) *Biochemistry 33*, 8167−8171.
Richarz, R., Sehr, P., Wagner, G., & Wüthrich, K. (1979) *J. Mol. Biol. 130*, 19−30.
Rico, M., Bruix, M., Santoro, J., Gonzalez, C., Neira, J. L., Nieto, J. L., & Herranz, J. (1989) *Eur. J. Biochem. 183*, 623−638.

Robertson, A. D., & Baldwin, R. L. (1991) *Biochemistry 30*, 9907−9914.
Roder, H. (1989) *Methods Enzymol. 176*, 446−473.
Roder, H., Wagner, G., & Wüthrich, K. (1985) *Biochemistry 24*, 7396−7407.
Santoro, J., González, C., Bruix, M., Neira, J. L., Nieto, J. L., Herranz, J., & Rico, M. (1993) *J. Mol. Biol. 229*, 722−734.
Santoro, M. M., Liu, Y., Khan, S. M. A., Hou, L.-X., & Bolen, D. W. (1992) *Biochemistry 31*, 5278−5283.
Somero, G. N. (1986) *Am. J. Physiol. 251*, 197−213.
Timasheff, S. N. (1993) *Annu. Rev. Biophys. Biomol. Struct. 22*, 67−97.
Udgaonkar, J. B., & Baldwin, R. L. (1988) *Nature 335*, 694−699.
Udgaonkar, J. B., & Baldwin, R. L. (1990) *Proc. Natl. Acad. Sci. U.S.A. 87*, 8197−8201.
Wagner, G., & Wüthrich, K. (1979) *J. Mol. Biol. 134*, 75−94.
Wagner, G., & Wüthrich, K. (1982) *J. Mol. Biol. 160*, 343−361.
Wlodawer, A., Svensson, L. A., Sjölin, L., & Gilliland, G. L. (1988) *Biochemistry 27*, 2705−2717.
Woodward, C. K., & Hilton, B. D. (1980) *Biophys. J. 32*, 561−575.
Woodward, C. K., Simon, I., & Tuchsen, E. (1982) *Mol. Cell. Biochem. 48*, 135−160.
Wüthrich, K., & Wagner, G. (1979) *J. Mol. Biol. 130*, 1−18.
Yancey, P. H., Clark, M. E., Hand, S. C., Bowlus, R. D., & Somero, G. N. (1982) *Science 217*, 1214−1222.
Yao, M., & Bolen, D. W. (1995) *Biochemistry 34*, 3771−3781.

BI9516945